Ornamental Plant Research

ARTICLE

Open Access

https://doi.org/10.48130/OPR-2023-0004

Ornamental Plant Research **2023**, 3:4

Physiological and transcriptome analyses to infer regulatory networks in flowering transition of *Rosa rugosa*

Xiaobin Wang[1#], Fei Zhao[2#], Qikui Wu[1], Shutang Xing[2], Yunyan Yu[1*] and Shuai Qi[1*]

[1] *Shandong Provincial Research Center of Demonstration Engineering Technology for Urban and Rural Landscape, College of Forestry, Shandong Agricultural University, Tai'an 271018, China*

[2] *College of Horticulture Science and Engineering, Shandong Agricultural University, Tai'an 271018, China*

[#] These authors contributed equally: Xiaobin Wang, Fei Zhao

[*] Corresponding authors, E-mail: yxyxst@sdau.edu.cn; shuaiqi@sdau.edu.cn

Abstract

Rosa rugosa is a famous Chinese traditional flowering species with high economic value. Flowering transition is an important process in plant growth and development. Although characterization of the flowering transition process has made great progress in some plants such as model plants, the process in *R. rugosa* has not been rigorously characterized to establish a mechanism. In this study, the changes of buds during flowering transition in *R. rugosa* 'Duoji Huangmei' were analyzed through transcriptomic sequencing combined with morphological and physiological index determinations. Results showed that with the morphology changes of buds, both sugar and starch content showed a similar up-down pattern while phytohormones content displayed various trends, which implied that sugar, starch and phytohormones might play diverse roles during flowering transition in *R. rugosa*. Moreover, a total of 4363 differentially expressed genes (DEGs) were identified at three developmental stages. Among them, 74 DEGs were involved in metabolism, transport, and signal transduction of sugar, starch, and phytohormones, as well as photoperiod and vernalization response. We proposed that these DEGs were not regulated independently but interacted with each other to construct a gene-gene network to regulate flowering transition of *R. rugosa*, and the regulatory network from vegetative growth stage (S1) to flowering transition stage (S2) was more complicated. These results further enriched the study of flowering transition in *Rosa* and lay an important foundation for breeding new varieties with desired floral traits.

Citation: Wang X, Zhao F, Wu Q, Xing S, Yu Y, et al. 2023. Physiological and transcriptome analyses to infer regulatory networks in flowering transition of *Rosa rugosa*. *Ornamental Plant Research* 3:4 https://doi.org/10.48130/OPR-2023-0004

INTRODUCTION

Flowering transition is a process in which the apical meristem gradually develops from the vegetative meristem to the reproductive meristem under the control of complicated genetic networks in response to the internal regulatory factors and external environmental factors[1]. To date, some progress has been made in the study on the molecular mechanism of flowering transition in some plants such as *Rosa*[2]. Foucher et al. identified 13 potential flowering regulatory genes(*RoRGA* , *RoSLY* , *RoSOC1* , *MASAKO B3* , etc.) in *R. hybrida* 'Black Baccara' related to flower development, gibberellin, and photoperiodic pathways through EST data[3]. It was found that overexpression of *FT* genes into *R. rugosa* 'Bao White' can significantly reduce the juvenile phase of the plant and enable it to flower earlier[4]. By transcriptome sequencing, Dubois et al. found that transcripts of the flowering integrator *RcSOC1* accumulate only during the growth stage and flower initiation stage, and are not expressed at the later stages of flowering[5]. Randoux et al. suggested that the expression of *RoKSN* was inhibited and resulted in the suppression of flowering when a high concentration of Gibberellic acid(GA) was applied to a season of flowering *R. chinensis*[6]. *R. rugosa* is a famous Chinese traditional flowering species with aromatic compounds and strong resistance to stress including cold, drought, pest, salt and alkali. However, the regulatory mechanism on the flowering transition of *R. rugosa* is still unclear. Accordingly, exploring the regulatory mechanism of flowering transition in *R. rugosa* can lay an important foundation for breeding new varieties with desired floral traits.

The process of flowering transition was regulated by the change of internal growth regulation substances, including carbohydrates and phytohormones[7]. Sugar molecules, such as sucrose, glucose, fructose, etc, are essential components of carbohydrates in plants, among which sucrose is the main form of long-distance carbohydrate transport in higher plants. As a flowering signal, sucrose is also involved in regulating transport efficiency, distribution of assimilated products, and the activation and repression of specific genes in plants[8]. Starch, which also belongs to carbohydrates, mainly generates sugar molecules through hydrolysis to provide the energy for the flowering transition in the plant. Relevant studies have shown that the decrease of amylose can exhibit a late-flowering phenotype[9]. Abscisic acid(ABA), Indole-3-acetic acid(IAA), and GA are all important phytohormones affecting plant growth and development, such as seed germination, stem elongation, flowering and fruiting, senescence and abscission, and dormancy, etc. Previous findings showed that the three phytohormones all play dual roles in regulating the flowering transition process of plants, namely promoting or inhibiting the flowering transition[10–12]. Light and temperature signals are important environmental factors affecting the flowering transition

process. Light regulates plant flower bud differentiation and flowering *via* the photoperiod pathway, an essential pathway for flowering in the plant[13]. The light signal of photoperiod is perceived by leaf, converted into biological signals and then transmitted to the flowering-time genes downstream to regulate the flowering transition process[14]. Nowadays, many studies on the impact of temperature on plant flowering have focused on vernalization, a phase of low temperature that some flowering species must undergo before flowering[15]. The molecular mechanisms underlying the vernalization response in *Arabidopsis thaliana* are well understood[16].

In this study, *R. rugosa* 'Duoji Huangmei', a novel continuous flowering cultivar, was selected as plant material. We explored the changes in morphology and content of sugar, starch, and phytohormones of buds during the flowering transition process. Furthermore, we conducted RNA sequencing (RNA-seq) to analyze the expression patterns of DEGs involved in the pathways related to sucrose, starch, IAA, ABA, GA, photoperiod, and vernalization. Finally, the molecular regulatory networks of flowering transition in *R. rugosa* was predicted.

MATERIALS AND METHODS

Plant material

R. rugosa 'Duoji Huangmei' was a diploid cultivar obtained by interspecific hybridization of *R. rugosa* and *R. xanthina*, which blooms from April to September. The tested *R. rugosa* 'Duoji Huangmei' plants were planted in the Rose Germplasm Nursery, Forestry Experimental Station of Shandong Agricultural University, Tai'an, China (36°10′15″ N, 117°09′25″ E), where they grew under natural conditions. Branches with buds of different sizes from nine different plants were selected randomly and then taken back to the laboratory on February 20th, 2021. After measuring the length using a vernier caliper, the buds were cut longitudinally. For the two halves of each cut bud, one half was used for observation to determine the developmental stage under Olympus SZX2-ILLT stereoscopic microscope (Olympus, Japan) and the other half at different developmental stages were quickly put into different tubes with liquid nitrogen and then stored at −80 °C for physiological index determination and transcriptome analysis. There were three biological replicates for each sample with 60~150 buds.

Determination of sugar and starch content

To measure the content of sugar and starch, a total of 200 mg samples were ground and homogenized in 8 mL of deionized water and placed in a boiling water bath for 30 min. After cooling to room temperature, the residue was filtered for subsequent starch content determination. The extracting liquid was transferred to the volumetric flask (25 mL) and the volume was fixed by distilled water, of which 0.5 mL extract liquid was transferred into the test tube. After 10 min of adding 1.5 mL distilled water, 0.5 mL anthrone-ethyl acetate solution (2%, *v/v*) reagent and 5 mL concentrated sulfuric acid (98%, *v/v*), the absorbance at 630 nm was read in a Beckman DU 800 UV–visible spectrophotometer (Beckman Coulter, USA) and compared to glucose standards.

The residue after centrifugation was transferred into a test tube with 10 mL distilled water and placed in a boiling water bath for 15 min. After adding 2 mL of 9.2 mol·L^{-1} perchloric acid for 2 min and then cooling to room temperature, the residue was filtered and the extracting liquid was transferred to the volumetric flask (25 mL) and the volume was fixed by distilled water. A total of 2 mL extracted liquid was collected to measure starch content at 620 nm using glucose as standards.

Determination of endogenous phytohormones content

The content of endogenous phytohormones in the buds were measured by high-performance liquid chromatography-mass spectrometry (HPLC-MS). A total of 500 mg samples were extracted overnight at 4 °C with 10 times the volume of acetonitrile solution and 2 μL internal standard master mix. The supernatant was collected by centrifugate at 12,000 rpm for 5 min at 4 °C. The obtained precipitate was added to 5 times the volume of acetonitrile solution and then extracted twice to combine the obtained supernatant. By adding 35 mg of C18 filler and vigorously shaking for 30 s, the supernatant was taken by centrifugate at 10,000 rpm for 5 min at 4 °C. Finally, it was dried with nitrogen, reconstituted with 200 μL methanol, passed through a 0.22 μm organic filter membrane, and placed in a −20 °C refrigerator for on-machine detection.

The HPLC-MS/MS analysis was conducted on a Poroshell 120 SB-C18 reversed-phase column (2.1 mm × 150 mm, 2.7 μm) at a flow rate of 0.3 mL·min^{-1} and a column temperature of 30 °C. Methanol / 0.1% formic acid (A) and water / 0.1% formic acid (B) were used as the mobile phase in gradient elution mode. The separation was performed using the following gradient: 20% for 1 min, from 20% to 50% in 2 min, from 50% to 80% in 6 min, at 80% for 1.5 min, then declining from 80% to 20% in 6s and 20% for 2.9 min. The injection volume is 2 μL. The ESI source operation parameters were as follows: ion source, ESI$^+$ and ESI$^-$; source temperature, 400 °C; ion spray voltage, +4,500 V and −4,000 V; curtain gas, 15 psi; atomization gas pressure, 65 psi; auxiliary gas pressure, 70 psi. Endogenous phytohormones were analyzed using scheduled multiple reaction monitoring (MRM).

Transcriptome analysis

Total RNA was extracted using the Total RNA Isolation Kit (Vazyme, China) according to the manufacturer's instructions. The quantity and quality of total RNA were assessed using 1% agarose gels and a NanoPhotometer® spectrophotometer (IMPLEN, USA). The integrity and concentration of total RNA were assessed using an Agilent 2100 RNA Nano 6000 Assay Kit (Agilent Technologies, USA) and Qubit®3.0 Fluorometer (Life Technologies, USA).

The poly(A) mRNA was isolated from total RNA through a NEBNext® Ultra™ RNA Library Prep Kit (New England Biolabs, China). After construction and normalization, three cDNA libraries were sequenced on the Illumina Hiseq 6000 Sequencing platform (Anoroad, China) and 150 bp paired-end reads were generated. The raw data were processed by removing the low-quality sequences (reads with more than 50% Q < 19 bases), the adaptor-pollute sequences, and sequences with ambiguous base reads accounting for more than 5%.

To understand their functions, the obtained clean reads were aligned to the *R. rugosa* genome database (http://eplantftp.njau.edu.cn/Rosa_rugosa/) by HISAT2 v2.1.0. The expression levels of genes were calculated as Fragments Per Kilobase of exon model per Million mapped fragments (FPKM), which eliminates the effect of sequencing depth and gene length on gene expression levels and permits direct data comparisons by the DESeq method[17]. The DEGs were identified if their

$\log_2$|Fold Change| was over 1 with a *q*-value ≤ 0.05. And then the GO (Gene Ontology, http://geneontology.org/) and KEGG (KyotoEncyclopediaofGenesandGenomes,www.kegg.jp)enrichment according to the identified DEGs were analyzed. The key DEGs involved in flowering transition were identified and their expression patterns were analyzed.

qRT-PCR verification

Quantitative real-time PCR (qRT-PCR) was carried out to verify the transcriptome data and analyze the expression patterns of 12 DEGs related to the flowering transition in *R. rugosa* 'Duoji Huangmei'. All actions were done on a CFX96 Real-time PCR System according to the instructions of the SYBR Green Pro Taq HS premixed qPCR kit (Accurate Biology, China). The amplification program was as follows: 30 s at 95 °C, 40 cycles of 5 s at 95 °C and 30 s at 60 °C. The relative expression level of differential genes was calculated by the $2^{-\Delta\Delta C_T}$ method with *RrGADPH* as an internal control. All primers used in this study are listed (Supplemental Table S1). All samples were repeated three times.

RESULTS

Morphology changes of buds

The bud length increased continuously during the flowering transition process of *R. rugosa* 'Duoji Huangmei' (Fig. 1a). The flowering transition process was divided into three stages, namely vegetative growth stage (S1), flowering transition stage (S2), and sepal primordial differentiation stage (S3). The bud length was less than 0.3 cm and the growth cone was pointed conical at S1 (Fig. 1b). Subsequently, the bud length increased to 0.3 cm ~ 0.5 cm, and the top of the growth cone gradually changed to oval at S2 (Fig. 1c). When the bud length was greater than 0.5 cm, the sepal primordium began to bulge, and the flowering transition process entered S3 (Fig. 1d).

Content changes of sugar and starch

Both sugar and starch content showed up-down patterns, peaking at S2 (Fig. 2a, b). The content of sugar had the highest level at S2 (122.85 mg·g^{-1}), and similar levels at S1 (94.37 mg·g^{-1}) and S3 (91.19 mg·g^{-1}). The content of starch increased from 5.55 mg·g^{-1} (S1) to 9.65 mg·g^{-1} (S2), and then decreased to 7.79 mg·g^{-1} at S3 stage (Fig. 2b). In addition, the content of sugar was about 13 times higher than that of starch at the same stage.

Content changes of endogenous phytohormones

The content of endogenous phytohormones presented diverse trends during the flowering transition of *R. rugosa* 'Duoji Huangmei'. The IAA concentration increased continuously with the contents from 0.79 ng·g^{-1} at S1 to 1.03 ng·g^{-1} at S2 and 1.25 ng·g^{-1} at S3 (Fig. 2c). The ABA content decreased 62.08% from S1 (293.92 ng·g^{-1}) to S2 (111.47 ng·g^{-1}) and then kept a gentle trend to S3 (135.22 ng·g^{-1}; Fig. 2d). The content of GA_1 and GA_3 had similar trends with valley values at S2. The GA_1 content maintained higher levels at S1 (1.05 ng·g^{-1}) and S3 (1.06 ng·g^{-1}) than that at S2 (0.77 ng·g^{-1}; Fig. 2e). However, the GA_3 content was much higher at S3 than the content at S1 and S2 (Fig. 2f). GA_4 content decreased continuously from 0.17 ng·g^{-1} at S1 to 0.10 ng·g^{-1} at S2, and 0.04 ng·g^{-1} at S3 (Fig. 2g). Taken together, total GA content showed higher levels at S1 (1.42 ng·g^{-1}) and S3 (0.92 ng·g^{-1}), and the lowest level at S2 (1.71 ng·g^{-1}; Fig. 2h).

Global analysis of RNA-seq data

Nine cDNA libraries were constructed to explore the key genes associated with the flowering transition in *R. rugosa* 'Duoji Huangmei'. And the raw data were deposited at the NCBI Sequence Read Archive (SRA) under accession numbers SRR21783417–SRR21783425. A total of 412,576,223 clean reads were obtained after removing the adaptor and low-quality reads (Supplemental Table S2). The Q20 and Q30 base rates were more than 96.45% and 91.17%, respectively. The average GC content was about 47.19%. The mapping rate of each library ranged from 76.28% to 77.51%. These results indicated that the sequencing quality was sufficient for further analyses.

GO and KEGG analyses of DEGs

There were 3676 DEGs identified from the compare combine of S2 *vs* S1, which included 2174 up-regulated genes and 1502 down-regulated genes (Fig. 3a). Taking S2 as control, a total of 1227 genes expressed differentially in S3, with more down-regulated genes (972) than up-regulated genes (255). Three thousand six hundred and six DEGs had different expression patterns between S3 and S1, including 2031 up-regulated genes and 1575 down-regulated genes. Five thousand three hundred and thirty two DEGs were found in three compare combinations, of which 417 DEGs were present in all combinations (Fig. 3b).

For the GO annotation, 3109, 3053, and 2930 DEGs were enriched in cellular component (CC), molecular functions (MF), and biological processes (BP), respectively. The majority of

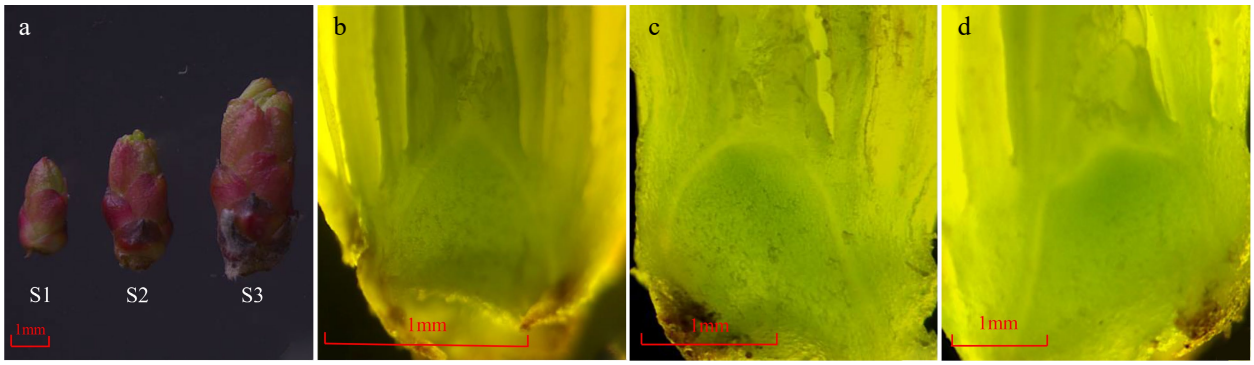

Fig. 1 The morphology changes of buds during the flowering transition process in *R. rugosa* 'Duoji Huangmei'. (a) The external morphology of buds at different development stages. (b) The growth cone was pointed conical at S1. (c) The growth cone was oval at S2. (d) The sepal primordium began to bulge at S3.

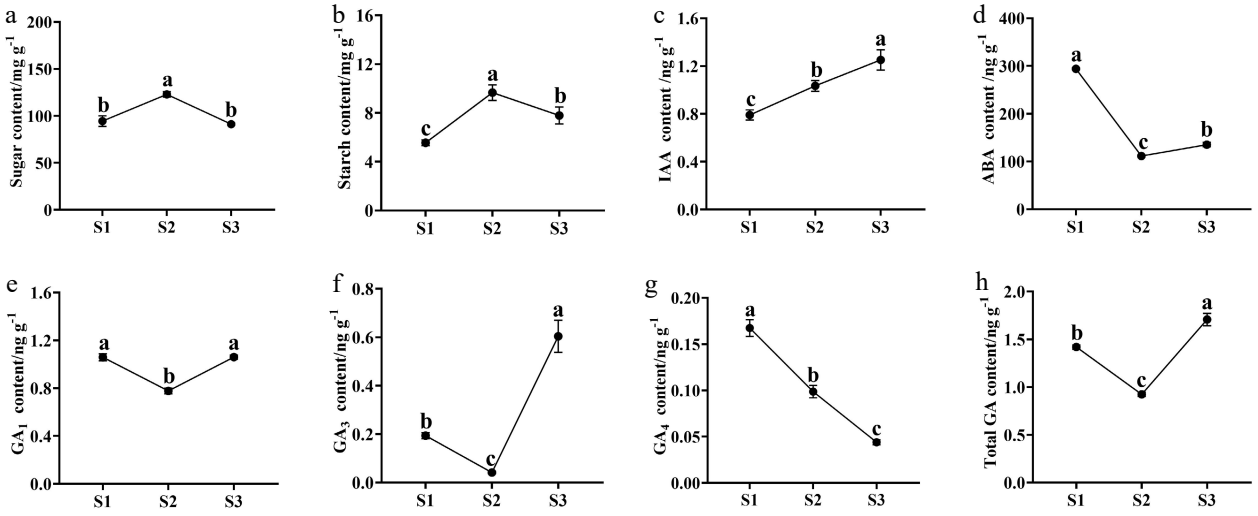

Fig. 2 The content changes of sugars, starch, and endogenous phytohormones in buds during the flowering transition process of *R. rugosa* 'Duoji Huangmei'. (a) Sugar content. (b) Starch content. (c) IAA content. (d) ABA content. (e) GA_1 content. (f) GA_3 content. (g) GA_4 content. (h) Total GA content. The different small letter for each content indicated significant difference between germplasms at $\alpha = 0.05$.

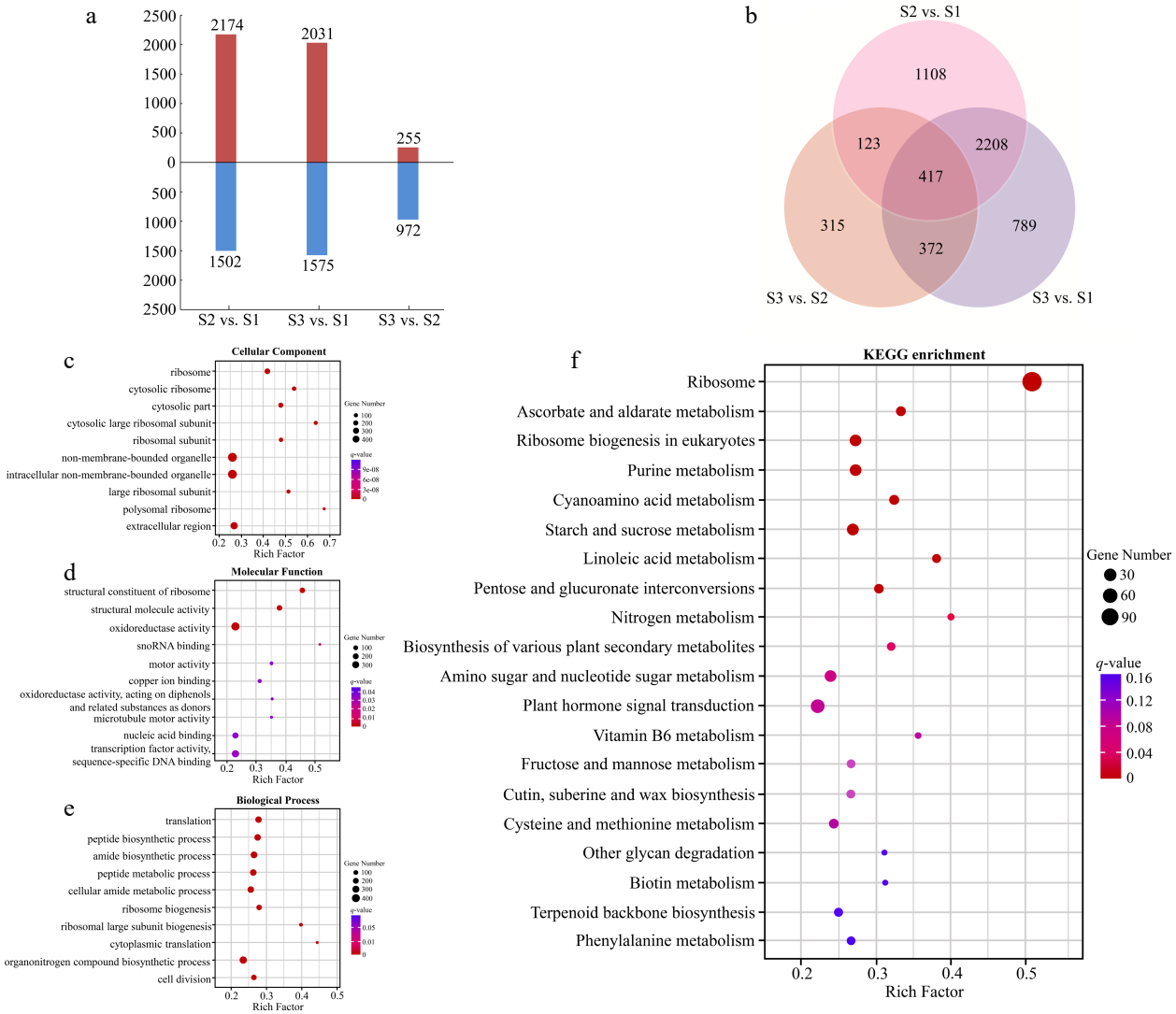

Fig. 3 Analyses of DEGs at three stages of flowering transition in *R. rugosa*. (a) Numbers of DEGs in each comparison. (b) Venn diagram analyses of differential and stage-specific expression genes in each comparison. (c) The GO terms of DEGs in the cellular components. (d) The GO terms of DEGs in the molecular functions. (e) The GO terms of DEGs in the biological process. (f) KEGG analysis of DEGs.

DEGs of CC category were assigned into 'Ribosome' (GO:0005840, 164 DEGs), 'Cytosolic ribosome' (GO:0022626, 92 DEGs), and 'Cytosolic part' (GO:0044445, 103 DEGs; Fig. 3c). For the MF category, the three most abundant structural constituents were 'Structural constituent of ribosome' (GO:0003735, 145 DEGs), 'Structural molecule activity' (GO:0005198, 168 DEGs), and 'Oxidoreductase activity' (GO:0016491, 394 DEGs; Fig. 3d). The three most abundant sub-categories divided from the BP category were 'Translation' (GO:0006412, 183 DEGs), 'Peptide biosynthetic process' (GO:0043043, 195 DEGs), and 'amide biosynthetic process' (GO:0043604, 192 DEGs; Fig. 3e).

By KEGG analysis, 794 DEGs were enriched in 132 metabolic pathways (Fig. 3f). Among them, the three most significant pathways for enrichment are 'Ribosome' (ko03010, 119 DEGs), 'Ascorbate and aldarate metabolism' (ko00053, 16 DEGs), and 'Ribosome biogenesis in eukaryote' (ko03008, 28 DEGs). In addition, we also found two pathways related to the flowering transition, namely 'Starch and sucrose metabolism' (ko00500, 25 DEGs) and 'Plant hormone signal transduction' (ko04075, 41 DEGs).

Expression analysis of sucrose- and starch-related DEGs

A total of 17 DEGs involved in starch and sucrose metabolism and transport were identified during the flowering transition process of *R. rugosa* 'Duoji Huangmei', which including five DEGs related to sugar transport and 12 DEGs related to sugar and starch metabolism, respectively (Fig. 4). There was one down-regulated DEG (*RrTPS*: evm.TU.chr6.439) and 11 up-regulated DEGs in the combination of S2 *vs* S1. In the combination of S3 *vs* S2, the expression of all nine DEGs exhibited downward trends. In addition, there were four DEGs identified from both S2 *vs* S1 and S3 *vs* S2, i.e., *RrSUT14* (evm.TU.chr2.691), *RrTPS* (evm.TU.chr6.439), *RrTPP* (evm.TU.chr3.4724), and *RrBAM3* (evm.TU.chr5.2267). Among them, except the expression level of *RrTPS* decreasing continuously, the other three DEGs showed up-down expression patterns.

Expression analysis of IAA-related DEGs

One DEG involved in IAA metabolism (*RrYUCCA2*: evm.TU.chr5.4871) and two DEGs related to IAA transport (*RrAUX1*: evm.TU.chr5.185; *RrPIN1*: evm.TU.chr4.173) were discovered and presented up-regulated expression during the flowering transition process of *R. rugosa* 'Duoji Huangmei' (Fig. 5). A total of 11 DEGs involved in IAA signal transduction were distinguished. However, the expression trends of DEGs related to IAA signal transduction were complex, which was different from the highly consistent expression trends of DEGs associated to IAA metabolism and transport. In the combine of S2 *vs* S1, five DEGs related to IAA signal transduction showed up-regulated trends, i.e., *RrTIR1* (evm.TU.chr4.4951), *RrIAA13* (evm.TU.chr6.4429), *RrSAUR76* (evm.TU.chr2.1179), *RrSAUR78* (evm.TU.chr2.5004), and *RrGH3.6* (evm.TU.chr1.3329), and three DEGs related to IAA signal transduction showed down-regulated trends, namely *RrIAA16* (evm.TU.chr7.3988), *RrIAA17* (evm.TU.chr4.5430) and *RrSAUR32* (evm.TU.chr3.3449). In the combination of S3 *vs* S2, only one DEGs related to IAA signal transduction (*RrGH3.1*: evm.TU.chr2.2246) presented up-regulated expression trend and two DEGs related to IAA signal transduction (*RrIAA17*: evm.TU.chr2.4338; *RrARF*: evm.TU.chr4.5433) showed down-regulated expression trends.

Expression analysis of ABA-related DEGs

Two DEGs involved in ABA metabolism (*RrNCED3*: evm.TU.chr1.2533; *RrAO2*: evm.TU.chr4.1894) were identified during the flowering transition process of *R. rugosa* 'Duoji Huangmei', which both decreased sharply in the combination of S2 *vs* S1 (Fig. 6). There were nine DEGs related to ABA signal transduction in the combination of S2 *vs* S1, of which eight DEGs showed sharply down-regulated expression trends

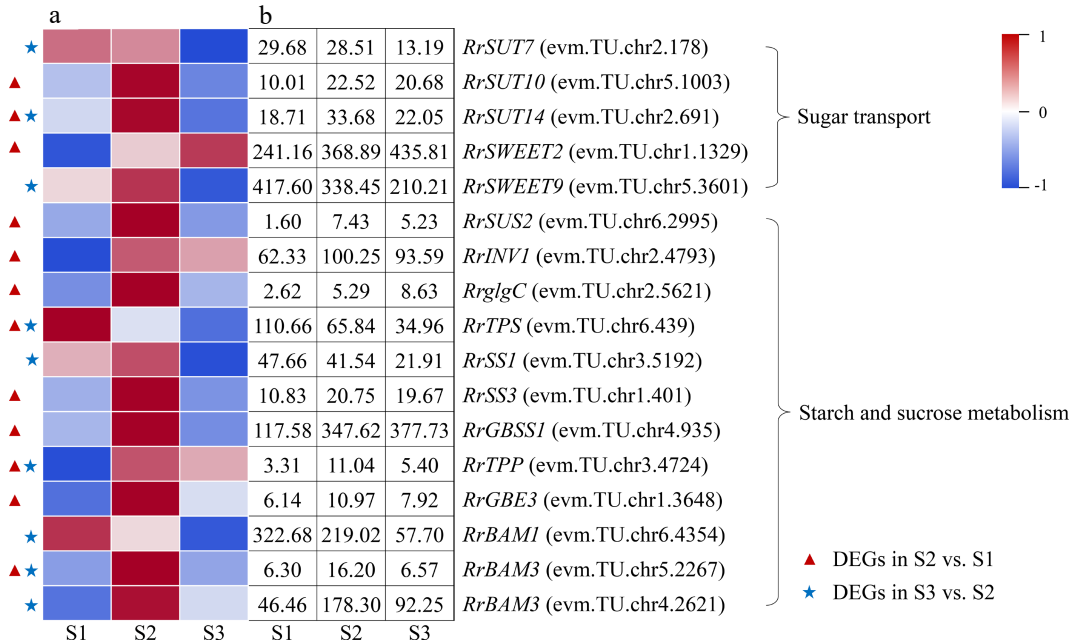

Fig. 4 Expression of starch- and sucrose-related DEGs. (a)The expression heat map of DEGs. (b) The FPKM values of DEGs. BAM: Beta-amylase; GBE3: 1,4-alpha-glucan-branching enzyme 3; GBSS1: Granule-bound starch synthase 1; glgC: Glucose-1-phosphate adenylyltransferase; INV1: insoluble isoenzyme CWINV1-like; SS1: Starch synthase 1; SUS2: Sucrose-phosphate synthase 2; SUT: Sugar transport protein; SWEET: Sugars will eventually be exported transporter; TPP: Trehalose-phosphate phosphatase; TPS: Trehalose-phosphate synthase

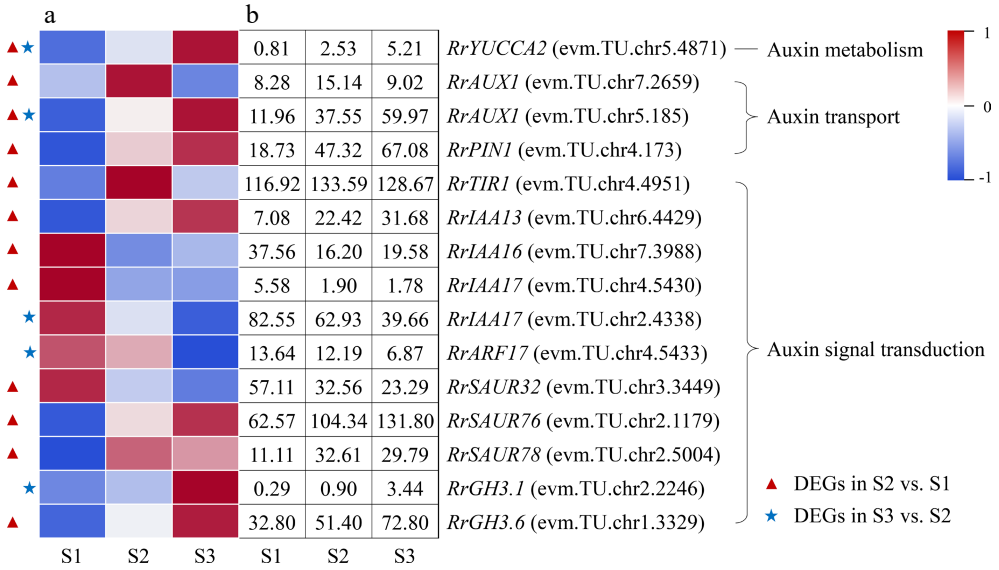

Fig. 5 Expression of IAA-related DEGs. (a) The expression heat map of DEGs. (b) The FPKM values of DEGs. ARF: Auxin response factor; AUX1: Auxin 1; GH3: Gretchen hagen 3; PIN1: PIN-formed acicular protein 1; SAUR: Small auxin-up RNA protein; TIR1: Transport inhibitor response protein 1;YUCCA2: YUCCA flavin-containing monooxygenase 2

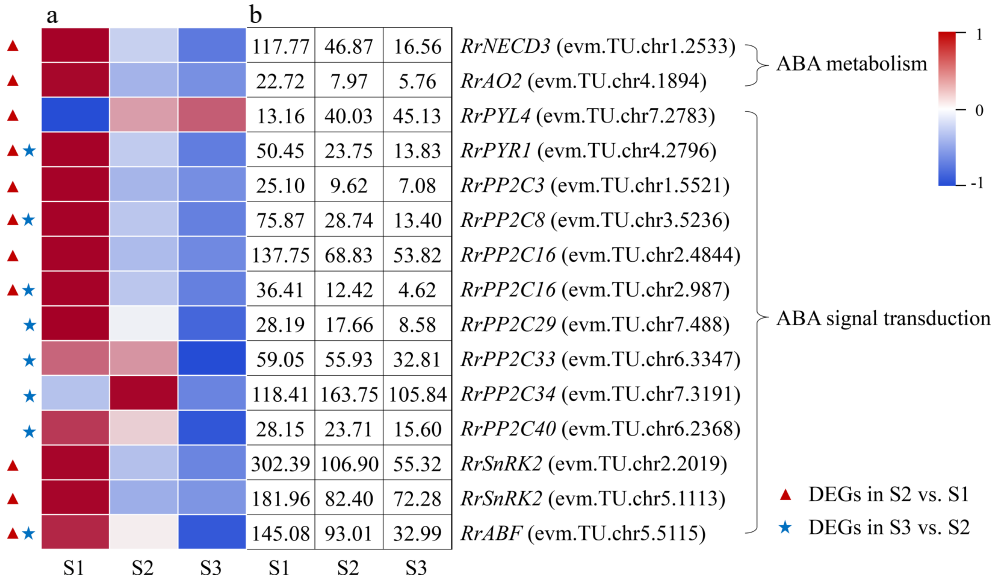

Fig. 6 Expression of ABA-related DEGs. (a) The expression heat map of DEGs. (b) The FPKM values of DEGs. ABF: ABA responsive element binding factor; AO2: Aldehyde oxidase 2; NECD3: 9-cis-epoxycarotenoid dioxygenase 3; PP2C: Protein phosphatase 2C; PYL4: Pyrabactin resistance-like 4 protein; PYR1: Pyrabactin resistance 1 protein; SnRK2: Sucrose nonfermenting 1-related protein kinase 2

except *RrPYL4* (evm.TU.chr7.2783). Furthermore, eight DEGs associated to ABA signal transduction were selected from the combination of S3 *vs* S2, which showed slight downward expression patterns from S2 to S3. In addition, four DEGs, namely *RrPYR1* (evm.TU.chr4.2796), *RrPP2C8* (evm.TU.chr3.5236), *RrPP2C16* (evm.TU.chr2.987), and *RrABF* (evm.TU.chr5.5115), were present in both S2 *vs* S1 and S3 *vs* S2.

Expression analysis of GA-related DEGs

Two DEGs associated with GA metabolism, *RrGA2ox1* (evm.TU.chr1.2534) and *RrGA3ox1* (evm.TU.chr2.4322), were distinguished and both exhibited down-regulated expression trends during the flowering transition process of *R. rugosa* 'Duoji Huangmei' (Fig. 7). And the former one was identified as DEG in combinations of both S2 *vs* S1 and S3 *vs* S2, which expression continued to decline. A total of 14 DEGs related to GA signal transduction were identified during the flowering transition process. Interestingly, 12 of 14 DEGs were present in the combination of S2 *vs* S1, of which nine DEGs showed up-regulated expression trends and three DEGs (*RrGID1A*: evm.TU.chr7.3415; *RrSnakin-2*: evm.TU.chr5.4611; *RrSCL1*: evm.TU.chr5.2181) showed downward patterns. Unlike the combination of S2 *vs* S1, there were only six DEGs identified in the combine of S3 *vs* S2, and all of them showed down-regulated expression trends.

Expression analysis of photoperiod- and vernalization-related DEGs

A total of seven DEGs associated with photoperiod were annotated during the flowering transition process of *R. rugosa*

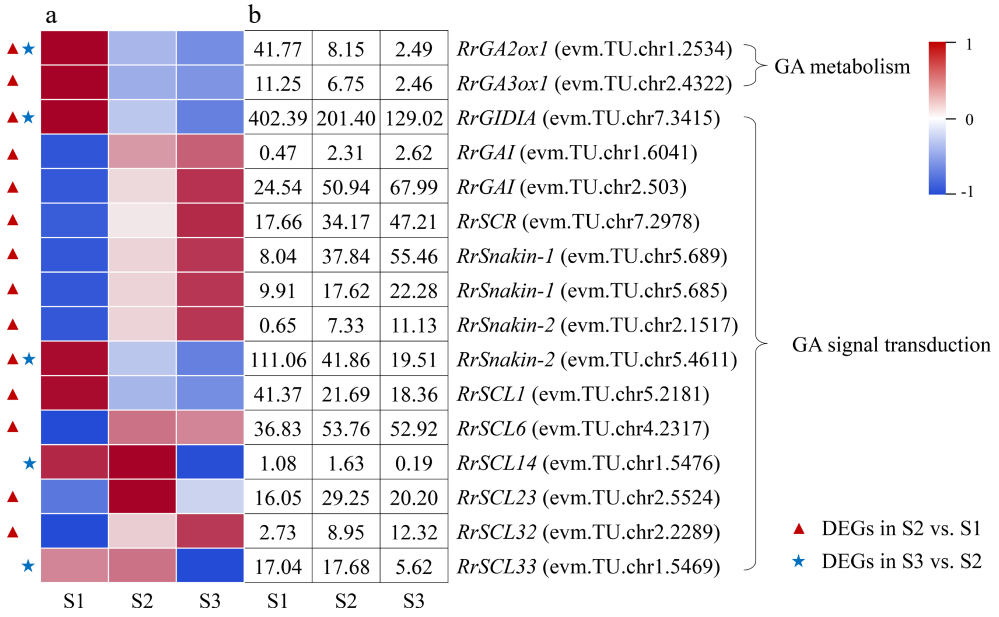

Fig. 7 Expression of GA-related DEGs. (a) The expression heat map of DEGs. (b) The FPKM values of DEGs. GA2ox1: Gibberellin 2-beta-dioxygenase 1; GA3ox1: Gibberellin 3-oxidase 1; GAI: GA insensitive protein; GID1A: GA insensitive dwarf 1 protein; SCL: Scarecrow-like protein; SCR: Scarecrow protein

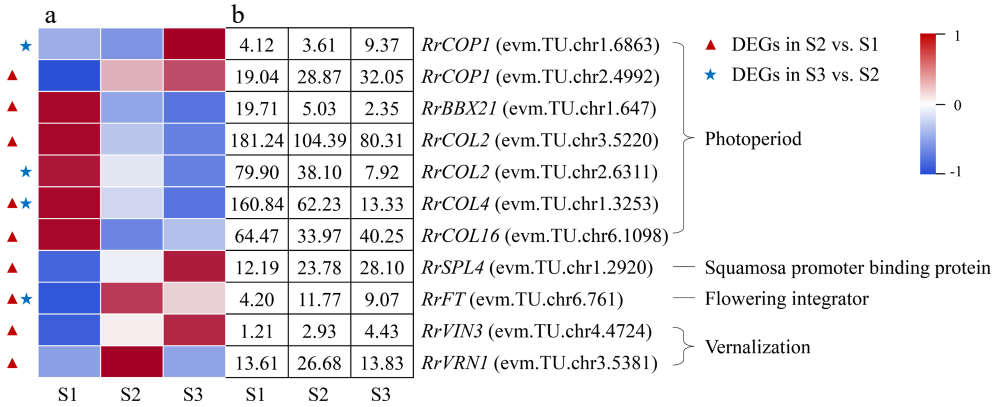

Fig. 8 Expression of photoperiod- and vernalization-related DEGs. (a) The expression heat map of DEGs. (b) The FPKM values of DEGs. BBX21: B-box 21; CO: CONSTANS; COL: CONSTANS-like; COP1: Constitutive Photomorphogenesis 1; FLC: Flowering Locus C; FT: Flowering locus T protein; SPL4: Squamosa promoter-binding-like protein 4;VIN3: Vernalization insensitive protein 3; VRN1: Vernalization protein 1

'Duoji Huangmei', of which five and three DEGs were found in the combination of S2 *vs* S1 and S3 *vs* S2, respectively (Fig. 8). Four of the five DEGs in the combination of S2 *vs* S1, i.e., *RrBBX21* (evm.TU.chr2.4992), *RrCOL2* (evm.TU.chr3.5220), *RrCOL4* (evm.TU.chr1.3253), and *RrCOL16* (evm.TU.chr6.1098) showed down-regulated expression trends, and one DEG (*RrCOP1*: evm.TU.chr2.4992) had an up-regulated expression pattern. One of the three DEGs in the combination of S3 *vs* S2, *RrCOP1* (evm.TU.chr1.6863), had an up-regulated expression trend, while the other three DEGs showed down-regulated expression sharply. In addition, two DEGs involved in vernalization (*RrVRN1*: evm.TU.chr3.5381; *RrVIN3*: evm.TU.chr4.4724) were identified, which only presented in the combination of S2 *vs* S1 and showed up-regulated expression. It must be mentioned that the florigen gene *FT* is a critical regulator in the flowering transition of plants. One *RrFT* gene was annotated in this study, i.e., evm.TU.chr6.761, whose expression level presented an up-down trend during the flowering transition process.

qRT-PCR validation

In this experiment, a total of 12 genes related to the starch and sucrose metabolism (*RrSUT14*, *RrTPP*, *RrTPS*), IAA metabolism and signal transduction (*RrYUCCA2*, *RrAUX1*), GA metabolism and signal transduction (*RrGA2ox1*, *RrGID1A*), ABA metabolism and signal transduction (*RrPYR1*, *RrPP2C16*, *RrABF*), photoperiod (*RrCOL4*), and the florigen gene *RrFT* were selected for qRT-PCR verification. As shown in Fig. 9, the expression trends of these genes were similar to those of transcriptome sequencing, and the correlation coefficients were all greater than 0.87. The results showed that the RNA-seq data were accurate and reliable.

DISCUSSION

Sugar and starch metabolism during flowering transition process of *R. rugosa*

In higher plants, sugar and starch play roles as both energy substances and flowering signals to regulate the floral

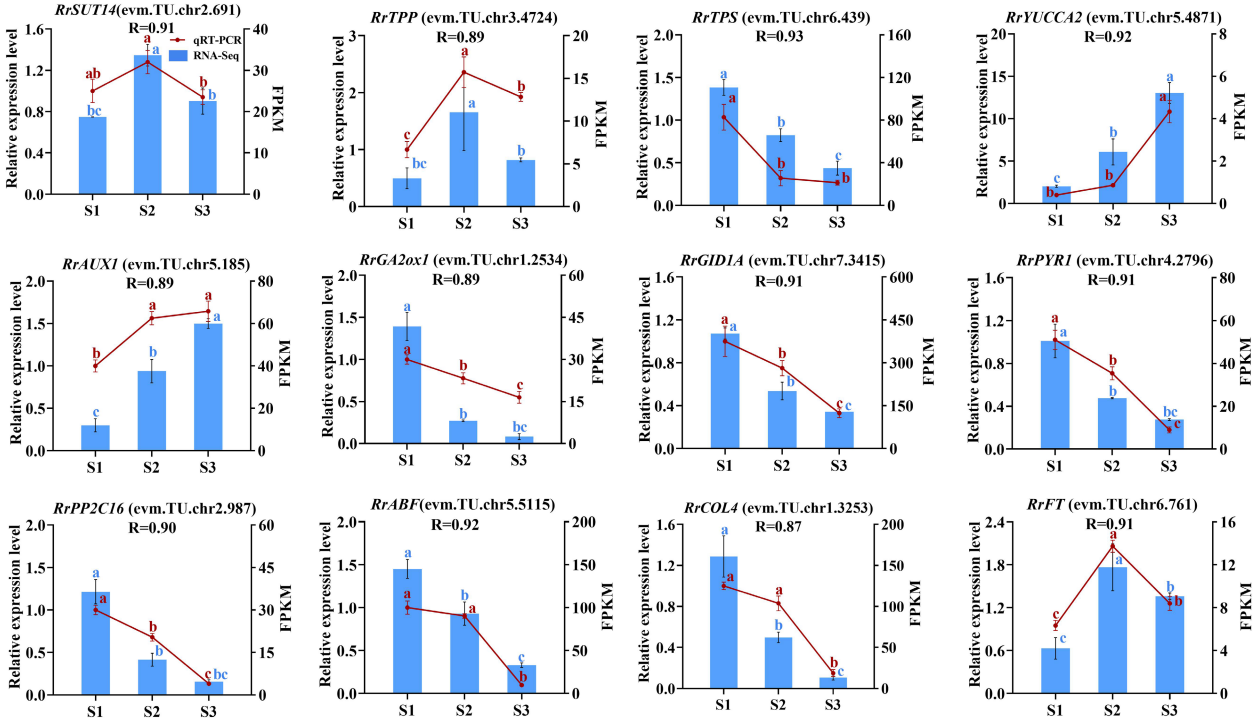

Fig. 9 The correlation of 12 genes between RNA-seq and qRT-PCR data. Letters on the error line indicate significant differences. The different lower case letters for each expression level indicated significant difference between germplasms at $\alpha = 0.05$.

transition process[18]. The content of sugar and starch both presented up-down or continuous increased trends during flowering transition process[19,20], which predicted that the accumulation of sugar and starch probably can promote early phase of flowering transition in plants. In this study, we found that the content of sugar and starch both showed up-down patterns (Fig. 2a, b), consisted with the expression patterns of most related DEGs showng up-regulated in the combination of S2 *vs* S1 (Fig. 4). In addition, three DEGs (*RrSWEET2*: evm.TU.chr1.1329; *RrSUT10*: evm.TU.chr5.1003; *RrSUT14*: evm.TU.chr2.691) involved in sugar transport presented up-regulated expression in the combination of S2 *vs* S1. Previous studies showed that over expression of *MdSUT2* and *SWEET10* in *A. thaliana* resulted in early flowering, and the flowering transition of *pSuT* mutants was delayed significantly[21–23]. Accordingly, we speculated that the flowering transition process from S1 to S2 in *R. rugosa* was promoted by the co-expression of three DEGs involved in sugar transport and ten DEGs related to sugar and starch metabolism, such as *RrSUS2* (evm.TU.chr6.2995), *RrglgC* (evm.TU.chr2.5621), *RrTPS* (evm.TU.chr6.439), etc. In addition, the expression of all nine DEGs were downward trends in the combination of S3 *vs* S2, including three sugar transport-related genes (*RrSWEET9*: evm.TU.chr5.3601; *RrSUT7*: evm.TU.chr2.178; *RrSUT14*: evm.TU.chr2.691) and six sugar and starch metabolism-related genes (*RrTPS*: evm.TU.chr6.439; *RrTPP*: evm.TU.chr3.4724; *RrSS1*: evm.TU.chr3.5192; *RrBAM1*: evm.TU.chr6.4354; *RrBAM3*: evm.TU.chr4.2621; *RrBAM3*: evm.TU.chr5.2267). This indicated that the flowering transition process from S2 to S3 may not require large amounts of sugar and starch. Previous studies showed that the expression of genes related to sugar and starch metabolism also gradually increases during the flowering transition process in *Malus domestica* and *Fragaria* × *ananassa*. This indicated that Rosaceae plants may regulate the flowering transition process by accumulating sufficient sugars and starch[24,25].

IAA metabolism, transport, and signal transduction during the flowering transition process of *R. rugosa*

For most plants, the content of IAA presented continuous increased or up-down trends during flowering transition process and exogenous IAA treatment can promote or restrain plant flowering transition[12,26]. In this study, the content of IAA increased continually during the floral transition process (Fig. 2c). Relevant studies also indicated that IAA content also continued to increase during the flowering transition in *R. odorata* var. *gigantea* and *Crocus sativus*[27,28]. And only one DEG involved in IAA biosynthesis, *RrYUCCA2* (evm.TU.chr5.4871), was identified and its expression level presented continually increased trend during the whole flowering transition process, which was consistent with the change in the content of IAA (Fig. 5). IAA was synthesized in the cytoplasm, but its content in cells was determined by multiple IAA transporters, such as PINs, AUX1/LAXs, and ABCBs, etc[29]. In this study, the expression levels of one output transport DEG (*RrPIN1*: evm.TU.chr4.173) and two input transport DEGs (*RrAUX1*: evm.TU.chr5.185; *RrAUX1*: evm.TU.chr7.2659) increased in the combination of S2 *vs* S1. Accordingly, we speculated that the increased expression levels of *RrPIN1* and *RrAUX1* may induce the spatiotemporal variation of IAA content in cells and then affect the expression of IAA responsive genes in IAA signal transduction pathway. IAA signal transduction pathway was consisted of IAA receptor (*TIR1/AFB*), transcriptional repressor (*AUX/IAA*), IAA response factor (*ARF*) and downstream target genes[30]. In this study, the expression of IAA receptor gene *RrTIR1* (evm.TU.chr4.4951) was up-regulated in the combination of S2 *vs* S1, which was probably promoted by the change of IAA content. Subsequently, three transcriptional repressor DEGs with

differential expressions (*RrIAA13*: evm.TU.chr6.4429; *RrIAA16*: evm.TU.chr7.3988; *RrIAA17*: evm.TU.chr4.5430) transduced IAA signals to *RrSAUR32* (evm.TU.chr3.3449), *RrSAUR76* (evm.TU.chr2.1179), *RrSAUR78* (evm.TU.chr2.5004), and *RrGH3.6* (evm.TU.chr1.3329) *via* non-differential expressed IAA response gene *RrARF* during the early stage of flowering transition.

Taken together, the changes of IAA content during flowering transition of many plants have a strong regularity, which indicates that IAA may be closely related to flowering transition. Many genes involved in IAA metabolism, transport and signal transduction pathways have also been identified, but have not been proved to directly affect the flowering transition process. Therefore, the effect of IAA-related genes on flowering transition is worthy of further study.

ABA metabolism and signal transduction during flowering transition process of *R. rugosa*

Relevant studies have shown that the content of ABA presented down-up trends during the floral transition process and exogenous ABA treatment can restrain plant flowering transition in most plants[31]. In this study, we found that the ABA content decreased 62.08% from S1 to S2 and then kept a gentle up trend to S3 (Fig. 2d), which was consistent with many Rosaceae plants, such as *R. odorata* var. *gigantea* and *Prunus avium*[27,32]. Furthermore, the expression levels of two ABA synthesis-related genes (*RrNECD3*: evm.TU.chr1.2533; *RrAO2*: evm.TU.chr4.1894) decreased significantly and exhibited no significant difference in the combination of S2 *vs* S1 and S3 *vs* S2, respectively, which was consistent with the change of ABA content (Fig. 6). Subsequently, ABA signals were transducted *via* PYR/PYL/RCAR-PP2C-SnRK2 pathway to activate downstream targets such as transcription factors and ion channels, triggering an ABA response[33]. In this study, we found that the expression trends of most DEGs involved in the PYR/PYL/RCAR-PP2C-SnRK2 signal transduction pathway were consistent with ABA content. Up to now, no other genes involved to PYR/PYL/RCAR-PP2C-SnRK2 signal transduction pathway have been proved to directly affect the flowering transition process, except of *BrABF3* in *Brassica rapa* var. *chinensis* which promotes flowering through the direct activation of *CO* transcription[34]. Related studies indicated a potential regulatory role for ABA signalling in the flowering time of *Eriobotya japonica*[35]. Therefore, direct evidence is needed to prove that ABA content and genes related to ABA metabolism and signal transduction have direct impact on flowering transition of *R. rugosa*.

GA metabolism and signal transduction during flowering transition process of *R. rugosa*

The total GA content presented down-up or up-down trends during flowering transition process in different plants and exogenous GA treatment can regulate plant flowering transition[28,36]. In this study, total GA content showed the lowest level at S2 (Fig. 2h), which was consistent with the results in *Phalaenopsis aphrodite* and *Nelumbo nucifera*[37,38]. However, GA content showed a decreasing trend during the flowering transition in some Rosaceae plants[39–40]. It was noteworthy that GA_3 content presented a similar trend to total GA content (Fig. 2f), and we found that exogenous GA_3 treatment of different concentrations demonstrated significant effect on flowering transition of *R. rugosa* (in process), which indicated that GA_3 played an important role in GA effect on the flowering transition of *R. rugosa*.

Moreover, *GA3ox* catalyzes the production of active GA, while *GA2ox* catalyzes the conversion of active GA into inactive GA[41]. In this study, the down-regulated expression of *RrGA3ox1* (evm.TU.chr2.4322) may induce the decrease of GA content from S1 to S2, and the down-regulated expression of *RrGA2ox1* (evm.TU.chr1.2534) perhaps increased the GA content in the combine of S3 *vs* S2 (Fig. 7). Previous studies showed that GA content can affect the content of DELLA protein, which in turn led to changes in the expression of related genes inhibited or promoted by DELLA, showing GA signal response and regulating plant flowering transition finally[42]. In this study, there were 11 and four DEGs related to GA signal transduction in the combination of S2 *vs* S1 and S3 *vs* S2, respectively, which indicated that GA signal transduction were more complicated in the early stage of flowering transformation of *R. rugosa*. We speculated that the reduction in total GA content and the down-regulated expression of one GA receptor protein gene (*RrGID1A*: evm.TU.chr7.3415) increased the content of DELLA protein by promoting the expression of three DELLA family genes (*RrGAI*: evm.TU.chr1.6041; *RrGAI*: evm.TU.chr2.503; *RrSCR*: evm.TU.chr7.2978). After that, DELLA protein promoted the expression of four SCL family genes (*RrSCL1*: evm.TU.chr5.2181; *RrSCL6*: evm.TU.chr4.2317; *RrSCL23*: evm.TU.chr2.5524; *RrSCL32*: evm.TU.chr2.2289) and inhibited the expression of one GASA family gene (*RrSnakin-2*: evm.TU.chr5.4611) from S1 to S2.

Photoperiod- and vernalization-related genes expression during the flowering transition process of *R. rugosa*

Photoperiod induces floral transition in plants by the changes in circadian rhythms. *CO* is an important element of the plant photoperiod regulatory pathway, which integrates light and circadian clock signals and delivers them to the flowering integron *FT* to regulate plant flowering transition[43]. However, CO family genes play diversified roles, namely promoting, inhibiting, or no effect on flowering transition[44,45]. *COP1* promotes *CO* degradation at the post-transcriptional level[46]. In this study, the up-regulated expression of two *COP1* genes (evm.TU.chr2.4992; evm.TU.chr1.6863) and the down-regulated expression of four *COL* genes (evm.TU.chr3.5220; evm.TU.chr1.3253; evm.TU.chr6.1098; evm.TU.chr2.6311) may cause a continuous decrease in CO protein content during flowering transition process, which suggested that CO protein acted as an inhibitor to the flowering transition in *R. rugosa*.

Temperature is an important factor affecting plant flowering, and most plants require a certain period of low-temperature induction before flowering, namely vernalization. The *VRN* gene play an important role during the vernalization process, which can inhibit the expression of *FLC*, an essential gene in the vernalization pathway, thereby promote flowering[47]. In this study, there was no DEG related to vernalization in the combination of S3 *vs* S2, which suggested that vernalization only acts at the early stage of flowering transition of *R. rugosa*. In the combination of S2 *vs* S1, the expression of both *RrVRN1* (evm.TU.chr3.5381) and *RrVIN3* (evm.TU.chr4.4724) showed up-regulated trends, but the expression of *RrFLC* genes were not detected. It was indicated that *RrVRN1* (evm.TU.chr3.5381) perhaps affected the flowering transition of *R. rugosa* by promoting directly the expression of *RrFT* (evm.TU.chr6.761), which was consistent with *Triticum aestivum*[48].

Hypothetical gene regulatory network construction

The regulatory network of flowering transition in higher plants is complex and comprehensive with the effect of many factors. The sugar and starch can both provide energy and act as a flowering signal to regulate the flowering transition pathway. IAA, ABA and GA can regulate the flowering transition both independently and in interaction with each other. Relevant studies indicated that the expression of *TPS* is induced by ABA[49]. In combination with the dynamic changes of ABA, the continuous decrease of *RrTPS* expression level may be influenced by ABA content. Trehalose-6-phosphate(T6P) can act as a flowering signal to indirectly activate the expression of *SPL*, and then *SPL* indirectly activates the expression of *FT*[50]. The expression of *RrSPL* and *RrFT* were up-regulated from S1 to S2, which indicated that there may be a positive regulatory relationship among T6P, *RrSPL*, and *RrFT*. The IAA-inducible protein SAUR inhibits the activity of PP2C-type protein phosphatase to regulate the plant growth and development process, which makes IAA to interact with ABA to regulate flowering transition in plants[51]. Up-regulated expression of *RrSAUR* and down-regulated expression of *RrPP2C* from S1 to S2 indicated that *RrPP2C* perhaps was negatively regulated by *RrSAUR*. The interaction between IAA and ABA is also reflected in the regulatory role of *ARF* on *ABF*. *ARF* can regulate downstream IAA-responsive genes and can regulate the expression of *ABF* in the ABA signaling transduction pathway, which in turn affects ABA signaling[52]. The expression trends of *RrARF* and *RrABF* were consistent during the flowering transition in *R. rugosa*, suggesting that down-regulation of *RrARF* expression drives down-regulation of *RrABF* expression. *DELLA* can bind directly to *CO* through its CCT structural domain and prevent *CO* from binding to the *FT* promoter[42]. *BBX21* can interact with *COP1* to regulate plant photomorphogenesis[53]. From S1 to S2, *RrDELLA* and *RrCOP1* were up-regulated in expression, and *RrCO* was down-regulated in expression, which indicated that *RrCO* may be repressed by *RrCOP1* and *RrDELLA*. In *A. thaliana*, *VRN1* and *VIN3* are involved in suppressing the negative regulation of *FT* by *FLC*. However, *RrFLC* with any expression levels in this study was not detected, which may be induced by suppression of *RrVRN1* and *RrVRN3* to *RrFLC*. Related studies indicated that *VRN1* can act directly with *FT*[48]. The expression trends of *RrVRN1* and *RrFT* were consistent from S1 to S2, indicating that the up-regulated expression of *RrFT* is due to the direct effect of *RrVRN1*. In addition, *RrFT* can integrate signals from multiple pathways, such as starch and sugar metabolism, vernalization and photoperiodic, to regulate the flowering transition of *R. rugosa* as a central gene.

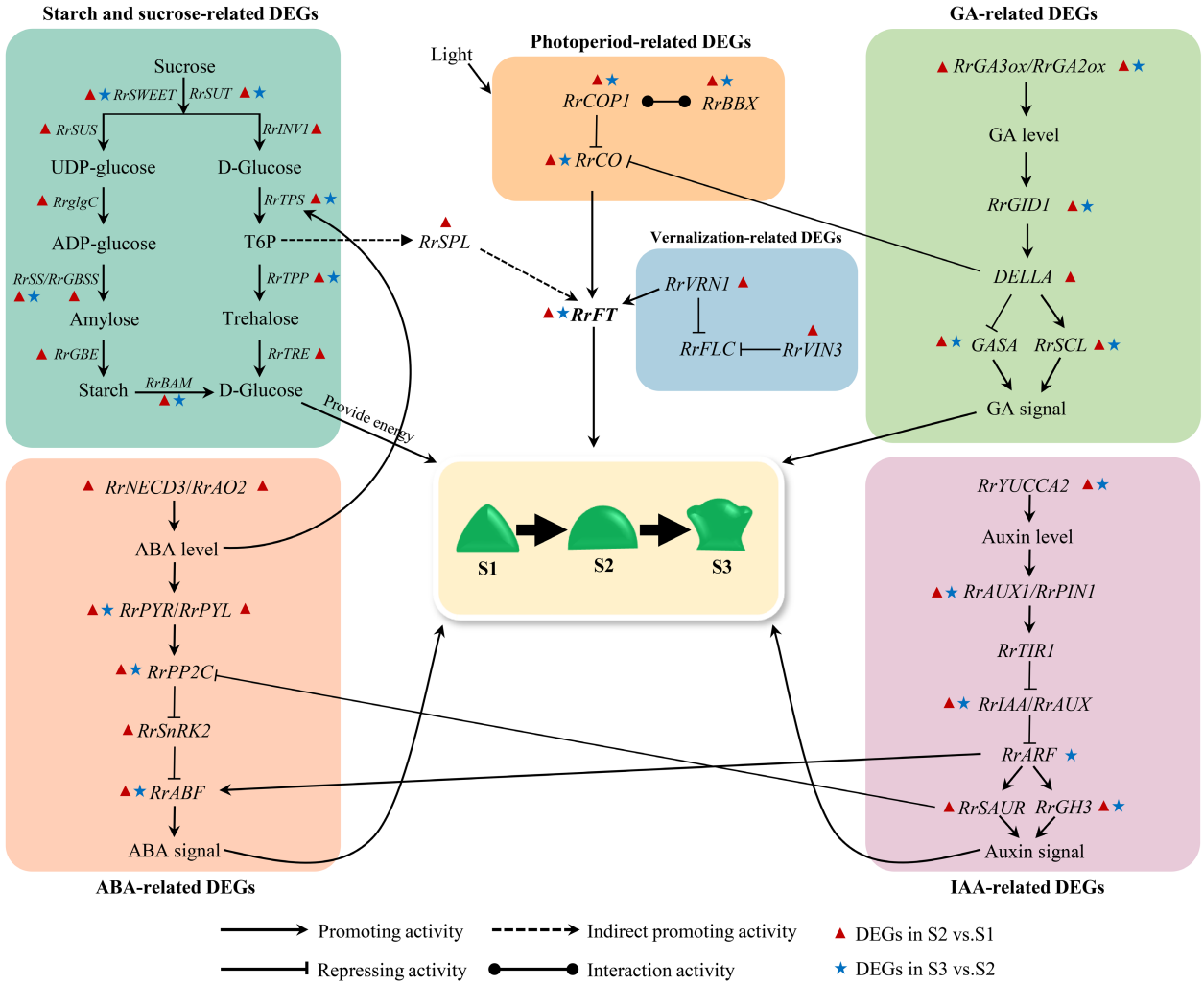

Fig. 10 Hypothetical model for the gene regulatory network of flowering transition in *R. rugosa*.

Based on the above results and previous research results, we constructed a hypothetical gene regulatory network map of flowering transition in *R. rugosa* 'Duoji Huangmei' (Fig. 10). In the network map, we proposed that 74 DEGs related to starch and sucrose (*RrSUT7/10/14*, *RrSWEET2/9*, *RrSUS2*, *RrglgC*, *RrSS1/3*, *RrGBSS1*, *RrGBE3*, *RrBAM1*,*RrBAM3*, *RrINV1*, *RrTPS*, *RrTPP*), IAA (*RrYUCCA2*, *RrPIN1*, *RrAUX1*, *RrTIR1*, *RrIAA13/16/17*, *RrSAUR32/76/78*, *GH3.1/3.6*), ABA (*RrNECD3*, *RrAO2*, *RrPYR1*, *RrPYL4*, *RrPP2C3/8/16/29/33/34/40*, *RrSnRK2*, *RrABF*), GA (*RrGA2ox1*, *RrGA3ox1*, *RrGID1A*, *RrGAI*, *RrSCR*, *Rrsnakin-1/2*, *RrSCL1/6/23/32/33*), photoperiod (*RrBBX21*, *RrCOL2/4/16*, *RrCOP1*), and vernalization (*RrVRV1*, *RrVIN3*) did not act independently but interact with each other to regulate flowering transition of *R. rugosa*. Moreover, we found that more DEGs presented in the combination of S2 *vs* S1 compared with the combination of S3 *vs* S2. Accordingly, we speculated that the gene regulatory network from S1 to S2 was more complicated during flowering transition of *R. rugosa*.

ACKNOWLEDGMENTS

This project was funded by the Shandong Agricultural Seeds Engineering Project (2020LZGC011) and the National Science Foundation of China (NSFC) (31870688).

Conflict of interest

The authors declare that they have no conflict of interest.

Supplementary Information accompanies this paper at (https://www.maxapress.com/article/doi/10.48130/OPR-2023-0004)

Dates

Received 26 October 2022; Accepted 9 February 2023; Published online 27 February 2023

REFERENCES

1. Davila-Velderrain J, Martinez-Garcia JC, Alvarez-Buylla ER. 2016. Dynamic network modelling to understand flowering transition and floral patterning. *Journal of Experimental Botany* 67:2565–72
2. Blümel M, Dally N, Jung C. 2015. Flowering time regulation in crops—what did we learn from Arabidopsis? *Current Opinion in Biotechnology* 32:121–29
3. Foucher F, Chevalier M, Corre C, Soufflet-Freslon V, Legeai F, et al. 2008. New resources for studying the rose flowering process. *Genome* 51:827–37
4. Xing W, Wang Z, Wang X, Bao M, Ning G. 2014. Over-expression of an *FT* homolog from *Prunus mume* reduces juvenile phase and induces early flowering in rugosa rose. *Scientia Horticulturae* 172:68–72
5. Dubois A, Carrere S, Raymond O, Pouvreau B, Cottret L, et al. 2012. Transcriptome database resource and gene expression atlas for the rose. *BMC Genomics* 13:638
6. Randoux M, Jeauffre J, Thouroude T, Vasseur F, Hamama, et al. 2012. Gibberellins regulate the transcription of the continuous flowering regulator, *RoKSN*, a rose *TFL1* homologue. *Journal of Experimental Botany* 63:6543–54
7. Silva LDS, Cavalcante ÍHL, da Cunha JG, Lobo JT, Carreiro DA, et al. 2022. Organic acids allied with paclobutrazol modify mango tree 'Keitt' flowering. *Revista Brasileira de Fruticultura* 44:e003
8. Cho LH, Pasriga R, Yoon J, Jeon JS, An G. 2018. Roles of sugars in controlling flowering time. *Journal of Plant Biology* 61:121–30
9. Cho LH, Yoon J, An G. 2017. The control of flowering time by environmental factors. *The Plant Journal* 90:708–19
10. Emami H, Kempken F. 2019. PRECOCIOUS 1 (POCO 1), a mitochondrial pentatricopeptide repeat protein affects flowering time in *Arabidopsis thaliana*. *The Plant Journal* 100:265–78
11. Guan H, Huang X, Zhu Y, Xie B, Liu H, et al. 2021. Identification of *DELLA* Genes and key stage for GA sensitivity in bolting and flowering of flowering Chinese cabbage. *International Journal of Molecular Sciences* 22:12092
12. Wang Y, Li B, Li Y, Du W, Zhang Y, et al. 2022. Application of exogenous auxin and gibberellin regulates the bolting of lettuce (*Lactuca sativa* L.). *Open Life Sciences* 17:438–46
13. Meng X, Li Y, Yuan Y, Zhang Y, Li H, et al. 2020. The regulatory pathways of distinct flowering characteristics in Chinese jujube. *Horticulture Research* 7:123
14. Cao S, Luo X, Xu D, Tian X, Song J, et al. 2021. Genetic architecture underlying light and temperature mediated flowering in *Arabidopsis*, rice, and temperate cereals. *The New phytologist* 230:1731–45
15. Luo X, He Y. 2020. Experiencing winter for spring flowering: A molecular epigenetic perspective on vernalization. *Journal of Integrative Plant Biology* 62:104–17
16. Lewandowska-Sabat AM, Fjellheim S, Rognli OA. 2012. The continental-oceanic climatic gradient impose clinal variation in vernalization response in *Arabidopsis thaliana*. *Environmental and Experimental Botany* 78:109–16
17. Love MI, Huber W, Anders S. 2014. Moderated estimation of fold change and dispersion for RNA-seq data with DESeq2. *Genome Biology* 15:550
18. Xue Y, Xue J, Ren X, Li C, Sun K, et al. 2022. Nutrient supply is essential for shifting tree peony reflowering ahead in autumn and sugar signaling is involved. *International Journal of Molecular Sciences* 23:7703
19. Mornya PMP, Cheng FY, Li HY. 2011. Chronological changes in plant hormone and sugar contents in cv. Ao-Shuang autumn flowering tree peony. *Horticultural Science* 38:104–12
20. Wu P, Wu C, Zhou B. 2017. Drought stress induces flowering and enhances carbohydrate accumulation in *Averrhoa Carambola*. *Horticultural Plant Journal* 3:60–66
21. Ma QJ, Hu DG, Lu J, Sun MH, Liu YJ, et al. 2016. Molecular cloning and functional characterization of the apple sucrose transporter gene *MdSUT2*. *Plant Physiology and Biochemistry* 109:442–451
22. Patzke K, Prananingrum P, Klemens PAW, Trentmann O, Rodrigues CM, et al. 2019. The plastidic sugar transporter pSuT influences flowering and affects cold responses. *Plant physiology* 179:569–587
23. Andrés F, Coupland G. 2012. The genetic basis of flowering responses to seasonal cues. *Nature Reviews Genetics* 13:627–39
24. Eshghi S, Tafazoli E, Dokhani S, Rahemi M, Emam Y. 2007. Changes in carbohydrate contents in shoot tips, leaves and roots of strawberry (*Fragaria* × *ananassa* Duch.) during flower-bud differentiation. *Scientia Horticulturae* 113:255–260
25. Xing LB, Zhang D, Li YM, Shen YW, Zhao CP, et al. 2015. Transcription Profiles Reveal Sugar and Hormone Signaling Pathways Mediating Flower Induction in Apple (*Malus domestica* Borkh.). *Plant & cell physiology* 56:2052–2068
26. Wu M, Wu J, Gan Y. 2020. The new insight of auxin functions: transition from seed dormancy to germination and floral opening in plants. *Plant Growth Regulation* 91:169–74
27. Guo XL, Yu C, Luo L, Wan HH, Zhen N, et al. 2018. Developmental transcriptome analysis of floral transition in *Rosa odorata* var. *gigantea*. *Plant Molecular Biology* 97:113–30
28. Hu J, Liu Y, Tang X, Rao H, Ren C, et al. 2020. Transcriptome profiling of the flowering transition in saffron (*Crocus sativus* L.). *Scientific Reports* 10:9680

29. Zwiewka M, Bilanovičová V, Seifu YW, Nodzyński T. 2019. The nuts and bolts of PIN auxin efflux carriers. *Frontiers in Plant Science* 10:985
30. Dubey SM, Serre NBC, Oulehlová D, Vittal P, Fendrych M, et al. 2021. No time for transcription-rapid auxin responses in plants. *Cold Spring Harbor Perspectives in Biology* 13:a039891
31. Guo Y, An L, Yu H, Yang M. 2022. Endogenous hormones and biochemical changes during flower development and florescence in the buds and leaves of *Lycium ruthenicum* Murr. *Forests* 13:763
32. Villar L, Lienqueo I, Llanes A, Rojas P, Perez J, et al. 2020. Comparative transcriptomic analysis reveals novel roles of transcription factors and hormones during the flowering induction and floral bud differentiation in sweet cherry trees (*Prunus avium* L. cv. Bing). *PLoS One* 15:e0230110
33. Hsu PK, Dubeaux G, Takahashi Y, Schroeder JI. 2021. Signaling mechanisms in abscisic acid-mediated stomatal closure. *The Plant Journal* 105:307–21
34. Zhang C, Zhou Q, Liu W, Wu X, Li Z, et al. 2022. *BrABF3* promotes flowering through the direct activation of *CONSTANS* transcription in pak choi. *The Plant Journal* 111:134–48
35. An H, Jiang S, Zhang J, Xu F, Zhang X. 2021. Comparative transcriptomic analysis of differentially expressed transcripts associated with flowering time of loquat (*Eriobotya japonica* Lindl.). *Horticulturae* 7:171
36. Qin L, Zhang X, Yan J, Fan L, Rong C, et al. 2019. Effect of exogenous spermidine on floral induction, endogenous polyamine and hormone production, and expression of related genes in 'Fuji'apple (*Malus domestica* Borkh.). *Scientific Reports* 9:12777
37. Li Z, Xiao W, Chen H, Zhu G, Lv F. 2022. Transcriptome analysis reveals endogenous hormone changes during spike development in *Phalaenopsis*. *International Journal of Molecular Sciences* 23:10461
38. Sheng J, Li X, Zhang D. 2022. Gibberellins, brassinolide, and ethylene signaling were involved in flower differentiation and development in *Nelumbo nucifera*. *Horticultural Plant Journal* 8:243–50
39. Yi X, Gao H, Yang Y, Yang S, Luo L, et al. 2021. Differentially expressed genes related to flowering transition between once-and continuous-flowering Roses. *Biomolecules* 12:58
40. Li Y, Zhang D, Zhang X, Xing L, Fan S, et al. 2018. A transcriptome analysis of two apple (*Malus* × *domestica*) cultivars with different flowering abilities reveals a gene network module associated with floral transitions. *Scientia Horticulturae* 239:269–81
41. Yoshida H, Takehara S, Mori M, Ordonio RL, Matsuoka M, et al. 2020. Evolution of GA metabolic enzymes in land plants. *Plant and Cell Physiology* 61:1919–34
42. Bao SJ, Hua CM, Shen LS, Yu H. 2020. New insights into gibberellin signaling in regulating flowering in *Arabidopsis*. *Journal of Integrative Plant Biology* 62:118–31
43. Karimi M, Ahmadi N, Ebrahimi M. 2022. Photoreceptor regulation of *Hypericum perforatum* L. (cv. Topas) flowering under different light spectrums in the controlled environment system. *Environmental and Experimental Botany* 196:104797
44. Kim SK, Park HY, Jang YH, Lee JH, Kim JK, et al. 2013. The sequence variation responsible for the functional difference between the CONSTANS protein, and the CONSTANS-like (COL) 1 and COL2 proteins, resides mostly in the region encoded by their first exons. *Plant Science* 199:71–78
45. Yang T, He Y, Niu S, Yan S, Zhang Y. 2020. Identification and characterization of the *CONSTANS* (*CO*)/*CONSTANS-like* (*COL*) genes related to photoperiodic signaling and flowering in tomato. *Plant Science* 301:110653
46. Ponnu J, Hoecker U. 2021. Illuminating the COP1/SPA ubiquitin ligase: fresh insights into its structure and functions during plant photomorphogenesis. *Frontiers in Plant Science* 12:662793
47. Ahmad S, Peng D, Zhou Y, Zhao K. 2022. The genetic and hormonal inducers of continuous flowering in orchids: An emerging view. *Cells* 11:657
48. Tanaka C, Itoh T, Iwasaki Y, Mizuno N, Nasuda S, et al. 2018. Direct interaction between VRN1 protein and the promoter region of the wheat *FT* gene. *Genes & Genetic Systems* 93:25–29
49. Tian L, Xie Z, Lu C, Hao X, Wu S, et al. 2019. The trehalose-6-phosphate synthase TPS5 negatively regulates ABA signaling in *Arabidopsis thaliana*. *Plant Cell Reports* 38:869–82
50. Ponnu J, Schlereth A, Zacharaki V, Działo MA, AbelC, et al. 2020. The trehalose 6-phosphate pathway impacts vegetative phase change in *Arabidopsis thaliana*. *The Plant Journal* 104:768–80
51. Ren H, Park MY, Spartz AK, Wong JH, Gray WM, et al. 2018. A subset of plasma membrane-localized PP2C. D phosphatases negatively regulate SAUR-mediated cell expansion in Arabidopsis. *PLoS Genetics* 14:e1007455
52. Matilla AJ. 2020. Auxin: hormonal signal required for seed development and dormancy. *Plants* 9:705
53. Xu D, Jiang Y, Li J, Lin F, Holm M, et al. 2016. BBX21, an *Arabidopsis* B-box protein, directly activates HY5 and is targeted by COP1 for 26S proteasome-mediated degradation. *PNAS* 113:7655–7660